



# Impact of triaxiality on the rotational structure of neutron-rich rhenium isotopes



M.W. Reed<sup>a,\*</sup>, G.J. Lane<sup>a</sup>, G.D. Dracoulis<sup>a</sup>, F.G. Kondev<sup>b</sup>, M.P. Carpenter<sup>c</sup>, P. Chowdhury<sup>d</sup>, S.S. Hota<sup>a</sup>, R.O. Hughes<sup>a</sup>, R.V.F. Janssens<sup>c</sup>, T. Lauritsen<sup>c</sup>, C.J. Lister<sup>c,d</sup>, N. Palalani<sup>a</sup>, D. Seweryniak<sup>c</sup>, H. Watanabe<sup>a,f</sup>, S. Zhu<sup>c</sup>, W.G. Jiang<sup>e</sup>, F.R. Xu<sup>e</sup>

<sup>a</sup> Department of Nuclear Physics, RSPE, Australian National University, Canberra, ACT 2601, Australia

<sup>b</sup> Nuclear Engineering Division, Argonne National Laboratory, Argonne, IL 60439, USA

<sup>c</sup> Physics Division, Argonne National Laboratory, Argonne, IL 60439, USA

<sup>d</sup> Department of Physics, University of Massachusetts Lowell, Lowell, MA 01854, USA

<sup>e</sup> School of Physics, Peking University, Beijing 100871, China

<sup>f</sup> RIKEN Nishina Center, 2-1 Hirosawa, Wako, Saitama 351-0198, Japan

## ARTICLE INFO

### Article history:

Received 7 July 2015

Received in revised form 17 November 2015

Accepted 20 November 2015

Available online 28 November 2015

Editor: D.F. Geesaman

### Keywords:

$\gamma$ -Ray spectroscopy

Neutron-rich

Shape transition

Triaxiality

## ABSTRACT

A number of 3-quasiparticle isomers have been found and characterised in the odd-mass, neutron-rich, <sup>187</sup>Re, <sup>189</sup>Re and <sup>191</sup>Re nuclei, the latter being four neutrons beyond stability. The decay of the isomers populates states in the rotational bands built upon the 9/2<sup>-</sup>[514] Nilsson orbital. These bands exhibit a degree of signature splitting that increases with neutron number. This splitting taken together with measurements of the M1/E2 mixing ratios and with the changes observed in the energy of the gamma-vibrational band coupled to the 9/2<sup>-</sup>[514] state, suggests an increase in triaxiality, with  $\gamma$  values of 5°, 18° and 25° deduced in the framework of a particle-rotor model.

© 2015 Published by Elsevier B.V. This is an open access article under the CC BY license (<http://creativecommons.org/licenses/by/4.0/>). Funded by SCOAP<sup>3</sup>.

## 1. Introduction

Neutron-rich rhenium isotopes ( $Z = 75$ ) and nuclei in the surrounding region are of considerable interest as they are predicted to exhibit significant changes in deformation, possibly leading to the emergence of triaxial shapes [1–4]. The experimental manifestations of triaxiality are expected to be subtle; for one-quasiparticle structures in odd- $A$  nuclei, the effects are principally reflected in the sign and magnitude of signature splitting in the rotational bands, and correlated effects in the  $M1$  and  $E2$  transition probabilities (see, for example, Refs. [5–7]). In the case of both single- and multi-quasiparticle states, triaxiality (and the associated  $\gamma$  vibrations) implies  $K$ -mixing, which will affect the properties of (nominally)  $K$ -forbidden decays. For example, in the tungsten isotopes ( $Z = 74$ ), a systematic decrease with neutron

number in the hindrances of decays from high- $K$  isomers has been attributed to effects linked to increasing axial asymmetry [8].

For transitional nuclei in this region, an additional challenge comes from their inherent softness. As a result, the shape is sensitive to the configuration as well as the driving effects of rotation. Furthermore, while  $K$ -mixing due to triaxiality could imply the presence of fewer or shorter-lived isomers, each case will depend on the details of the specific decay path and strengths and, in addition, to different mechanisms that can lead to isomers. For example, particularly long-lived, three-quasiparticle isomers have been identified in the  $Z = 77$  isotopes, <sup>191</sup>Ir and <sup>193</sup>Ir. These have been assigned triaxial configurations and the isomerism is predominantly due to spin trapping [9].

Previous work in even-even nuclei around  $Z = 75$  has not yet defined whether the low-lying structures are due to rigid-triaxial [10] or  $\gamma$ -unstable rotation [4,11]. Recent work suggests that neither of these models represents the definitive situation in these nuclei [12,13]. In odd- $A$  systems, the situation is further complicated by the addition of the unpaired particle/hole that can have deformation driving and polarising effects impacting the shape of

\* Corresponding author.

E-mail address: [matthew.reed@anu.edu.au](mailto:matthew.reed@anu.edu.au) (M.W. Reed).

the core. The present work documents the discovery of a number of new high- $K$  isomers in neutron-rich rhenium nuclei, the focus is on the level structures that are exposed by the decay of these long-lived states, and on how the properties of the low-lying bands provide comprehensive evidence for the development of triaxiality or  $\gamma$ -softness in neutron-rich rhenium nuclei.

Meyer-Ter-Vehn [14,15] has applied the particle-rotor framework to the interpretation of nuclei in this region of interest. Specifically, this work explored in detail the signature splitting and inversion in rotational level structures as a function of triaxiality [7,17–19]. The expectation of the model is that the energy of the one-quasiparticle configuration coupled to the  $\gamma$  vibration ( $1\text{-qp} \otimes 2_{\gamma}^{+}$ ) will decrease with increasing  $\gamma$  deformation, since the first  $2^{+}$  states in the even-even core (rotational,  $2_{1}^{+}$  and  $\gamma$ -vibrational,  $2_{2}^{+}$ ) are expected to have energies given by:

$$E_{2_{1,2}^{+}} = \frac{6\hbar^2}{2\mathcal{J}_0} \frac{9 \mp \sqrt{81 - 72\sin^2(3\gamma)}}{4\sin^2(3\gamma)} \quad (1)$$

where  $\mathcal{J}_0$  is an inertia parameter related to the magnitude of the deformation ( $\epsilon_2$ ) and the nucleon number ( $A$ ) [14,16] and the shape parameter,  $\gamma$ , that varies from  $0^\circ$  to  $60^\circ$  and relates to either prolate ( $0^\circ$ ), triaxial ( $\sim 30^\circ$ ) or oblate ( $60^\circ$ ) shapes. The effects of  $\gamma$  deformation on  $M1$  and  $E2$  matrix elements, mentioned earlier, will be reflected in the measured mixing ratios and  $g$  factors for transitions from rotational states. In this work a rigid-particle-rotor framework is applied, however, as mentioned earlier in regard to the even-even neighbours,  $\gamma$ -softness could certainly play a role.

In the present work, new results on the yrast states in  $^{187}\text{Re}$ ,  $^{189}\text{Re}$  and  $^{191}\text{Re}$  have been obtained from a series of measurements performed using deep-inelastic collisions [20] at Argonne National Laboratory. Three isotopically-enriched targets of  $44\text{ mg/cm}^2$   $^{192}\text{Os}$ ,  $7.5\text{ mg/cm}^2$   $^{187}\text{Re}$  and  $6\text{ mg/cm}^2$   $^{186}\text{W}$ , backed by 10, 25 and  $25\text{ mg/cm}^2$  Au deposits, respectively, were exposed to a  $\sim 6\text{-MeV/u}$   $^{136}\text{Xe}$  beam provided by the ATLAS accelerator facility. Emitted  $\gamma$  rays were observed using Gammasphere [21], an array of Compton suppressed hyper-pure germanium detectors. Two experimental configurations were employed. The first used a nanosecond-pulsed beam (825-ns separation between pulses), allowing for both in- and out-of-beam measurements. The bulk of the data were collected in this mode, where a minimum of three-fold coincidence events were required. The data were subsequently sorted into coincidence cubes and hypercubes for offline analysis. The second arrangement used a microsecond clock in conjunction with a chopped beam with different time periods ranging from microseconds to seconds. The main settings for the search for longer-lived isomers used beam on/off periods of 100/400  $\mu\text{s}$  and 1/4 ms, with 'prompt' two-fold coincidence events required. (A full list of time conditions is given in Ref. [9].) These data were sorted into time-dependent matrices for analysis.

## 2. Results

Previous studies of these isotopes include particle transfer for  $^{187}\text{Re}$ ,  $^{189}\text{Re}$  and  $^{191}\text{Re}$  [22,23], inelastic excitation of  $^{187}\text{Re}$  [24] and projectile fragmentation for  $^{191}\text{Re}$  [25,26]. The new level schemes are given in Fig. 1; these are based on prior-known level information as well on the new spectroscopic evidence such as double-gated  $\gamma$ -ray coincidence spectra (including coincident X rays for elemental assignments), total conversion coefficients from delayed intensity balances,  $\gamma$ - $\gamma$  angular correlations and lifetime information. Complete details on the level scheme construction will be presented elsewhere [29], while the present paper provides a more detailed explanation for only the most neutron-rich case of  $^{191}\text{Re}$ .

### 2.1. $^{191}\text{Re}$ level scheme and spin-parity assignments

Gamma rays depopulating an isomer with  $\tau = 111(48)\text{ }\mu\text{s}$  had been firmly assigned to  $^{191}\text{Re}$  in projectile fragmentation [25, 26], but the limited spectroscopic information meant that a level scheme was not proposed. These and other  $\gamma$  rays were observed in the present work (a representative double-gated  $\gamma$ -ray coincidence spectrum is shown in Fig. 2) and, from the high statistics coincidence data, a detailed level scheme for the yrast states in  $^{191}\text{Re}$  was constructed, see Fig. 1. Confirmation of the assignment to  $^{191}\text{Re}$  is further provided by the fact that the energies of the  $9/2^{-}$ [514] state and its first rotational band member were approximately known from transfer experiments [22,23], and match the 140-keV  $\gamma$  ray observed here.

Three band structures have been identified that are fed (indirectly) by isomeric states with respective lifetimes of  $\tau = 48(4)\text{ ns}$ ,  $101(58)\text{ ns}$  and  $73(5)\text{ }\mu\text{s}$  (see Fig. 3). The new lifetime of  $73(5)\text{ }\mu\text{s}$  is consistent with, but more precise than, the previous measurement [25,26]. The band structures are built on bandheads at 145, 414 and 621 keV. Assuming  $9/2^{-}$  for the bandhead at 145 keV (see Refs. [22,23]), the other bands have lowest levels with spins and parities of  $11/2^{-}$  and  $(13/2^{-})$ , with detailed arguments for these assignments presented below. The  $9/2^{-}$  and  $(13/2^{-})$  bands are assigned to the  $9/2^{-}$ [514] and  $9/2^{-}$ [514]  $\otimes 2_{\gamma}^{+}$  configurations, respectively. Very similar level structures with such assignments are observed in all three rhenium isotopes, as can be seen in Fig. 1. The band based on the  $11/2^{-}$  state at 414 keV is tentatively associated with the  $11/2^{-}$ [505] orbital and is only observed in  $^{191}\text{Re}$ .

The inferred conversion coefficient for the 116-keV transition from the 1602-keV, 73- $\mu\text{s}$  isomer to the  $21/2^{-}$  band member at 1486 keV (see Fig. 4), suggests an  $M1$  or  $E2$  character. Since no branch to the  $19/2^{-}$  band member at 1089 keV is observed, the 1602-keV level can be assigned as  $J^{\pi} = 25/2^{-}$ . The other branch from the 1602-keV state is the 94-keV transition to the 101-ns isomer at 1508 keV. Its conversion coefficient in Fig. 4 suggests an  $M2$  multipolarity, leading in turn to a  $21/2^{+}$  assignment for the state at 1508 keV. The angular correlation (Fig. 5) between its main decay branch of 419-keV and the 360-keV in-band stretched quadrupole transition, suggests a pure-stretched dipole character consistent with  $E1$  multipolarity and, hence, the  $J^{\pi} = 21/2^{+}$  assignment. Furthermore, the conversion coefficient for the 158-keV branch from the 1508-keV state to the 1350-keV level is consistent with an  $E1$  multipolarity (see Fig. 4), while the angular correlation between the 158-keV  $\gamma$  ray and the 460-keV stretched quadrupole transition in the  $11/2^{-}$ [505] band is consistent with a stretched-dipole character. This leads to the assignment of  $J^{\pi} = 19/2^{-}$  for the 1350-keV band member and, assuming a rotational sequence, a  $J^{\pi} = 11/2^{-}$  assignment for the 414-keV bandhead.

The 48-ns isomer at 1679 keV directly populates the  $21/2^{-}$  state of the  $9/2^{-}$  band via the 193-keV  $E1$  transition (confirmed through its conversion coefficient in Fig. 4). The absence of other de-excitation pathways to the  $9/2^{-}$  band leads to the suggested  $J^{\pi} = 23/2^{+}$  assignment. Also, a 171-keV  $\gamma$  ray is observed to precede in time the transitions below the 101-ns isomer at 1508 keV, confirming it as a branch from the 48-ns, 1679-keV  $23/2^{+}$  state.

In addition to the opportunity to propose spin/parity assignments, the measured angular correlations enable a direct determination of the  $M1/E2$  mixing ratios for the  $J \rightarrow J - 1$  in-band transitions in the  $9/2^{-}$ [514] bands in all of the rhenium nuclei under investigation. Fig. 5 provides an example, with  $\delta = 0.28_{-0.12}^{+0.14}$  obtained for the 140-keV transition in  $^{191}\text{Re}$ .

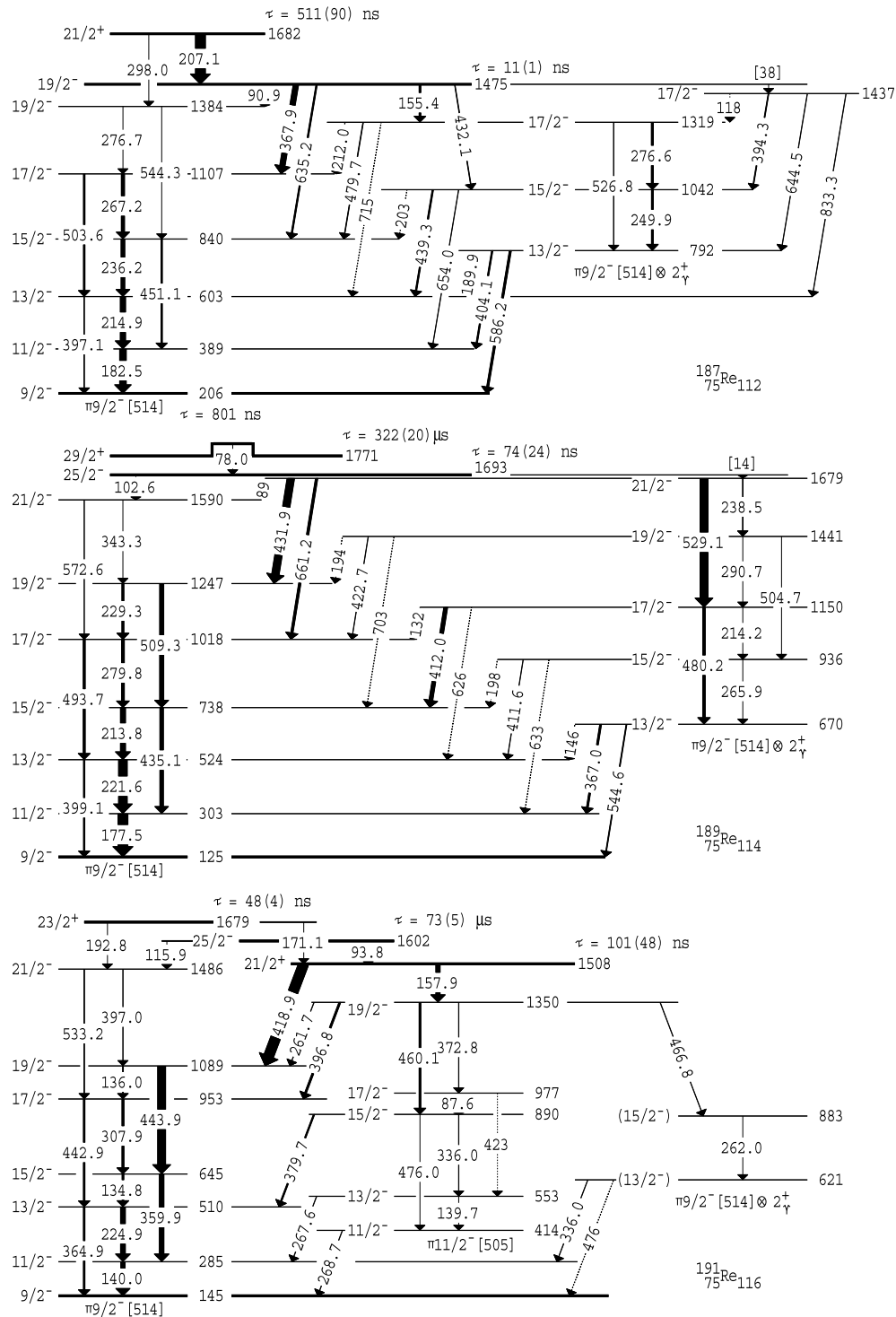


**Fig. 1.** Partial level schemes populated in the decays from isomeric states observed in  $^{187}\text{Re}$ ,  $^{189}\text{Re}$  and  $^{191}\text{Re}$ . The  $9/2^-$  levels in  $^{189}\text{Re}$  and  $^{191}\text{Re}$  are drawn with thicker lines to indicate the presence of unknown lifetimes expected because of the suggested multipolarity of transitions linking these states and the respective ground states. The current measurement is not sensitive to the single, isomeric transitions emitted from these expected long-lived states.

## 2.2. $^{187}\text{Re}$ and $^{189}\text{Re}$ level schemes and comparison with $^{191}\text{Re}$

A set of levels populated by the decay of an isomer in  $^{187}\text{Re}$  was reported by Shizuma et al. [24]. Much of their proposed scheme is confirmed here and numerous new transitions have been identified. The new information enabled firm spin-parity assignments to be proposed, resulted in a revised lifetime of 511(90) ns for the

isomer, measured previously as 164(33) ns, and the identification of a new 11(1)-ns isomeric level.

In the case of  $^{189}\text{Re}$ , only a few yrast states were identified earlier, including  $J = 9/2$  and  $J = 11/2$  levels at 125 and 303 keV respectively, from (t,  $\alpha$ ) reactions [23], resulting in an expected  $11/2^-$  to  $9/2^-$  in-band transition of 178(4) keV. The new  $^{189}\text{Re}$  level scheme in Fig. 1 is fed by two high-spin isomers that exhibit

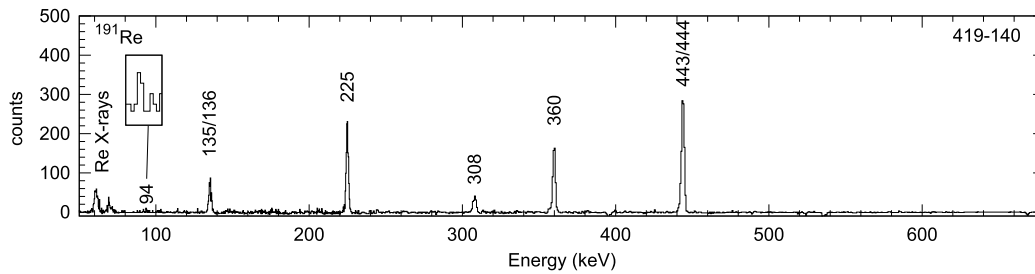


**Fig. 2.** Coincidence  $\gamma$ -ray spectrum for  $^{191}\text{Re}$  with a double gate on the 140-keV,  $11/2^- \rightarrow 9/2^-$  transition in the  $9/2^- [514]$  band and on the intense 419-keV transition feeding from the 101-ns isomer.

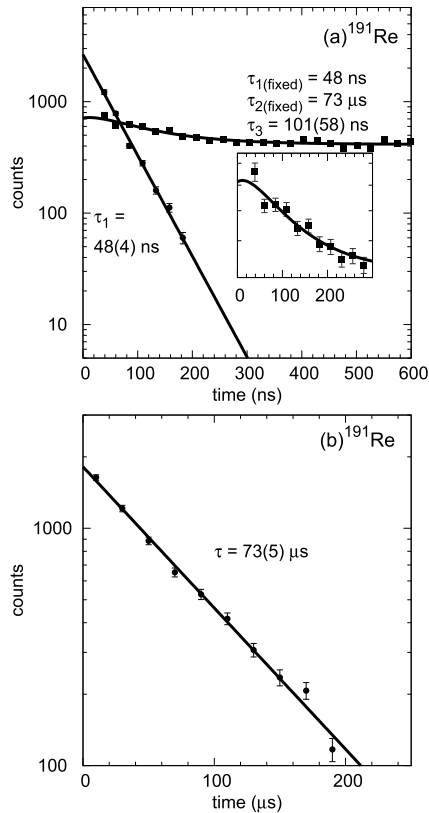


**Fig. 3.** Lifetime curves for isomers observed in  $^{191}\text{Re}$ ; (a) time spectra for  $^{191}\text{Re}$  showing the decay of the 48(4)-ns, 101(58)-ns and 73- $\mu\text{s}$  isomers. The 101(58)-ns curve has been fitted with fixed feeding components from the 48-ns and 73- $\mu\text{s}$  isomers; (b) time spectra taken with the 400- $\mu\text{s}$  chopped beam on the  $^{192}\text{Os}$  target, selecting the 73(5)- $\mu\text{s}$  isomer decay in  $^{191}\text{Re}$ .

lifetimes of 322(20)  $\mu\text{s}$  and 74(24) ns, with a match between the present  $11/2^-$  to  $9/2^-$   $\gamma$  energy of 177.5(1) keV. Not only does the  $\gamma$ -ray energy match that inferred from Ref. [23], but further evidence such as the observation of coincident Re X rays, coincident relationships with  $\gamma$  rays in partner nuclei (in deep-inelastic reactions, by observing in-beam prior to the decay of an isomeric state) and comparisons of relative yields from various targets, confirm the  $^{189}\text{Re}$  assignment.

In both  $^{187}\text{Re}$  and  $^{189}\text{Re}$ , two band structures have been identified, one built upon the  $9/2^- [514]$  proton orbital and another, with bandhead  $13/2^-$ , that has a pattern of interband decays to the  $9/2^- [514]$  band suggestive of a collective vibration. Therefore, this second band is proposed to be built upon the  $9/2^- [514] \otimes 2_1^+$  state in both nuclei. While only two states are observed in this band in  $^{191}\text{Re}$ , the similarities suggest the same assignment for the 621-keV state. The presence of the  $11/2^- [505]$  band in  $^{191}\text{Re}$  is discussed further below.

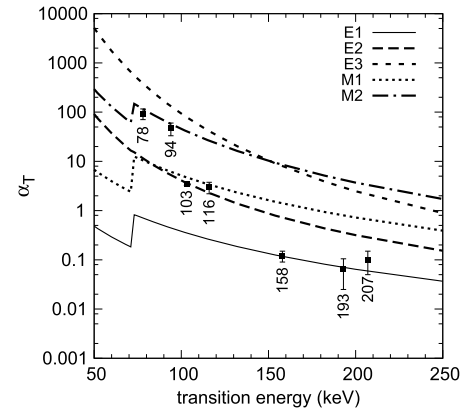


**Fig. 4.** Total conversion coefficients in  $^{187}\text{Re}$ ,  $^{189}\text{Re}$  and  $^{191}\text{Re}$  compared with predicted values [27]. Note that the total conversion coefficient value for the 78-keV transition was derived from the K-conversion coefficient measured through K-X-ray intensities [28] and scaled appropriately assuming M2 character.

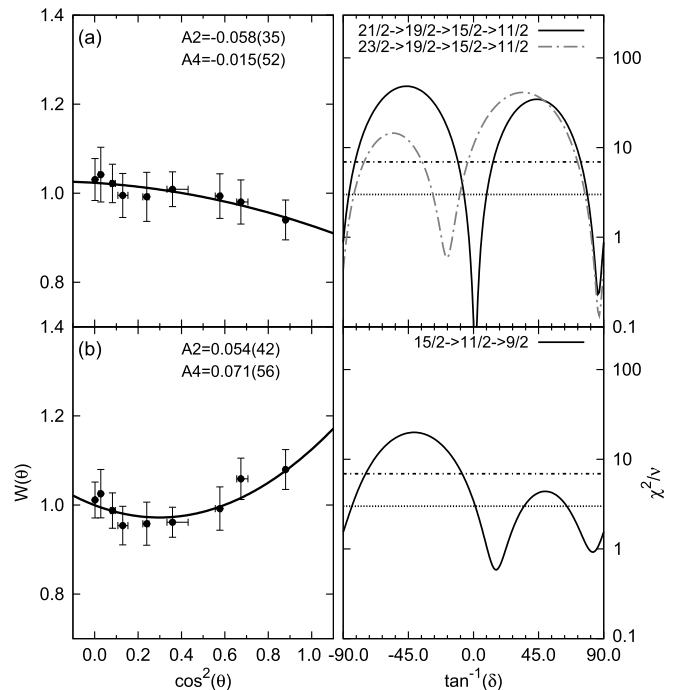


**Fig. 5.** Angular correlations between pairs of transitions in  $^{191}\text{Re}$ , specifically the 419/360-keV (top) and 360/140-keV pairs (bottom). Legendre polynomial fits to evaluate  $A_2$  and  $A_4$  coefficients are also given, together with  $\chi^2$  curves that indicate how well various spin sequences describe the angular correlation data. These can be used to determine the state spins, transition multiplicities and mixing ratios.

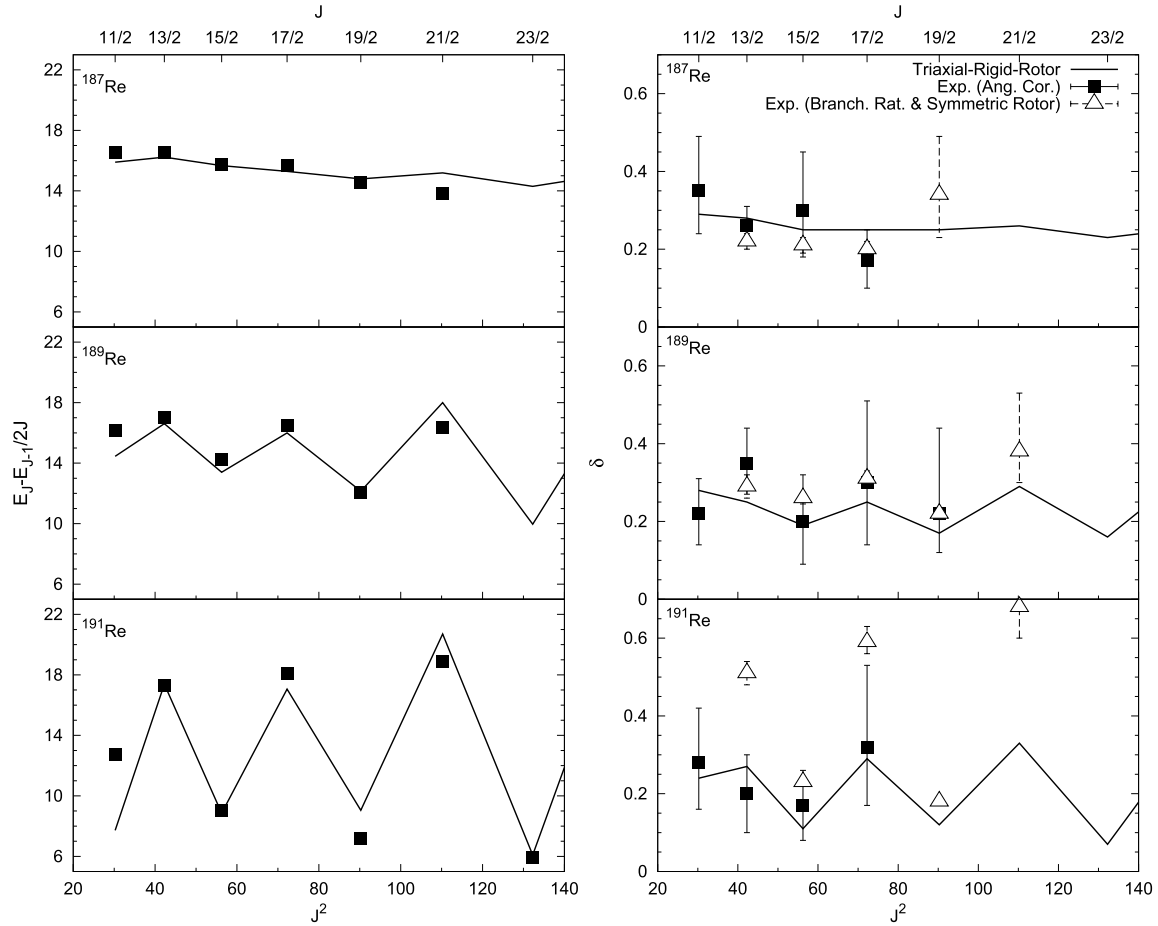


**Fig. 6.** Experimental moment of inertia parameters  $((E_J - E_{J-1})/2J$ , left panel) and mixing ratios  $(\delta$ , right panel) determined from  $\gamma\gamma$  angular correlations (solid squares), are compared with those predicted from a triaxial particle-rotor calculation (solid lines) as well as those evaluated from  $\gamma$  ray branching ratios with rotational formulas for axial rotors [32] (open triangles). In  $^{187}\text{Re}$  and  $^{191}\text{Re}$ , the level energy data points extend beyond those shown in the partial level schemes in Fig. 1. The higher-lying levels were observed in prompt-in-beam data on various targets [29].

### 3. Discussion and model calculations

Three experimental signatures in the present data set can be viewed as evidence for an increasing degree of triaxiality in the neutron-rich rhenium nuclei. In an axially symmetric nucleus, a rotational band built upon a high- $\Omega$  orbital is expected to exhibit interleaved states with regular spacings and no signature splitting. However, while minimal signature splitting in the  $9/2^-$  [514] band is present in  $^{187}\text{Re}$ , an increase is clearly visible in  $^{189}\text{Re}$ , with a further one in  $^{191}\text{Re}$ ; this can be seen from both the level schemes (see Fig. 1) and the filled square symbols in the left-hand panels of Fig. 6. This form of signature splitting is expected in nuclei with triaxial deformation [14].

Second, in even-even nuclei, the energy of the lowest  $2^+_\gamma$  vibrational state decreases as the degree of triaxiality increases (see equation (1)). In the present odd-mass systems, the equivalent observation is a fall in the energy difference between the  $9/2^-$  [514] and  $13/2^-$  ( $9/2^-$  [514]  $\otimes$   $2^+_\gamma$ ) bandheads, from 586 keV in  $^{187}\text{Re}$  to 545 keV in  $^{189}\text{Re}$  and 476 keV in  $^{191}\text{Re}$ . Furthermore, it is also worth noting that the lowest  $\gamma$ -vibrational state in even-even nuclei in the region occurs at 492 keV in  $^{192}\text{Os}$ , the isotone of  $^{191}\text{Re}$ . This lowering would be true whether the nucleus has a rigid-triaxial shape or is  $\gamma$  soft.

Third, the mixing ratios for the in-band  $M1/E2$  transitions in a triaxial rotor differ from those predicted for an axially symmetric one. Fig. 6 presents (filled squares) the experimental mixing ratios

for the cascade  $M1/E2$  transitions in the  $9/2^-$  [514] bands are determined in a model-independent way, from angular correlations. In an axially-deformed system, the mixing ratios can be deduced from the  $\gamma$ -ray intensity branching ratios between the  $J \rightarrow J-2$  and  $J \rightarrow J-1$  transitions. The results of this analysis are given as open triangles in Fig. 6. While there is a degree of overlap between the measured values and the calculations of the axially symmetric model for  $^{187}\text{Re}$  and  $^{189}\text{Re}$ , a marked divergence is noted for  $^{191}\text{Re}$ .

Taken together, these three experimental observations represent strong evidence for triaxial deformation developing in the neutron-rich rhenium nuclei. This, in turn, motivated an attempt to account for the observed properties with a particle-rotor model that includes the triaxial degree of freedom [30]. The approach consisted in reproducing not only the level spacing of the rotational bands, but also the in-band mixing ratios. Good agreement with experiment was obtained for the signature splitting, moments-of-inertia and in-band mixing ratios (see Fig. 6) with  $\gamma$  values of  $5^\circ$ ,  $18^\circ$ ,  $25^\circ$  and deformation parameters of  $\epsilon_2 = 0.23, 0.195, 0.18$  and  $\epsilon_4 = 0.093, 0.093, 0.080$  for  $^{187}\text{Re}$ ,  $^{189}\text{Re}$  and  $^{191}\text{Re}$ , respectively. Note a systematic decrease in  $\epsilon_2$ ,  $\epsilon_4$  deformation was required with increasing neutron number: this follows the general trend calculated (with axial symmetry only) by Möller et al. [31]. This decrease also provides a natural explanation for the observation of the  $11/2^-$  [505] band in  $^{191}\text{Re}$  only, as this level will approach the proton Fermi surface for a smaller  $\epsilon_2$  deformation.

The particle-rotor model also predicts the energy of the low-lying  $13/2^-$  vibrational bandhead, with values of 614, 551 and 461 keV calculated for the energy of the  $13/2^-$   $\gamma$ -vibrational states relative to the  $9/2^-$ [514] bandhead for  $^{187}\text{Re}$ ,  $^{189}\text{Re}$  and  $^{191}\text{Re}$ , respectively. Again, good agreement with experiment (586, 545 and 476 keV) is found. Finally, the decreasing energy of the  $9/2^-$ [514]  $\otimes 2^+_{\gamma}$  bandhead with increasing neutron number relative to the  $9/2^-$ [514] state is also consistent with Equation (1) and an increase in  $\gamma$  deformation of the even–even core. However, the model fails to reproduce the excited levels built upon the  $9/2^-$ [514]  $\otimes 2^+_{\gamma}$  bandhead.

Configuration-constrained potential energy surface (PES) calculations including the triaxial degree of freedom [2] were also carried out for 1-quasiparticle and 3-quasiparticle configurations to obtain the predicted deformations. The complete model calculation and configuration assignments for the isomers will be presented in Ref. [29]. Here, only the 1-quasiparticle states are discussed. Surprisingly, the  $9/2^-$ [514] configuration was found minimised in all cases at axial symmetry ( $\gamma \sim 0^\circ$ ). However, when supplemented by Total Routhian Surface (TRS) calculations, it became clear that rotation plays an important role in defining the degree of triaxiality. The TRS results were found to be qualitatively consistent with the conclusion from the triaxial particle-rotor calculations; e.g., with  $\gamma \sim 0^\circ$  in  $^{187}\text{Re}$ , while in the heavier isotopes there is a change at very low frequencies (via a  $\gamma$ -soft phase in  $^{189}\text{Re}$ ) to triaxiality in both  $^{189}\text{Re}$  ( $\gamma = -26^\circ$  at  $\hbar\omega = 0.150$  MeV) and  $^{191}\text{Re}$  ( $\gamma = -30^\circ$  at  $\hbar\omega = 0.1$  MeV).

#### 4. Conclusions

In this work, the isomer decays in  $^{187}\text{Re}$ ,  $^{189}\text{Re}$  and  $^{191}\text{Re}$  have been observed to populate members of both the  $9/2^-$ [514] rotational band and its associated  $\gamma$  vibration. Data on signature splitting,  $M1/E2$  mixing ratios of the  $9/2^-$ [514] in-band transitions and on the relative energies of the  $\gamma$ -vibrational bands all imply increasing  $\gamma$  deformation and the development of triaxiality with increased neutron number. In fact, some of the measured properties are consistent with those predicted by particle-triaxial-rotor calculations with values of  $\gamma = 5^\circ$ ,  $18^\circ$  and  $25^\circ$  for  $^{187}\text{Re}$ ,  $^{189}\text{Re}$  and  $^{191}\text{Re}$ , respectively. Nevertheless, given that the particle-rotor model fails to predict the excited levels built upon the  $9/2^-$ [514]  $\otimes 2^+_{\gamma}$  bandhead and that potential-energy surface calculations suggest increasing  $\gamma$ -softness for the heavier isotopes, one is led to the conclusion that the situation is somewhat more complex than a description in term of a rigid-triaxial shape. This is further suggested by TRS calculations showing that a degree of rotation is required to stabilise the  $\gamma$  deformation.

#### Acknowledgements

The authors are grateful to the accelerator team at ATLAS for their excellent contribution and to R.B. Turkentine for making the targets. G.J.L., G.D.D., and R.O.H. acknowledge travel support from Australian Government Access to Major Research Facilities Program Grant No. 06/07-H-04. This research was supported by grants from the Australian Research Council (DP0345844, DP0986725 and FT100100991) and by the U.S. Department of Energy, Office of Science, Office of Nuclear Physics, under contract number DE-AC02-06CH11357, and Grant No. DE-FG02-94ER40848. This research used resources of ANL's ATLAS facility, which is a DOE Office of Science User Facility.

#### References

- [1] P.D. Stevenson, et al., *Phys. Rev. C* 72 (2005) 047303.
- [2] P.M. Walker, F.R. Xu, *Phys. Rev. C* 74 (2006) 067303.
- [3] L.M. Robledo, R. Rodríguez, P. Sarriguren, *J. Phys. G* 36 (2009) 115104.
- [4] K. Nomura, T. Otsuka, R. Rodríguez, L.M. Robledo, P. Sarriguren, *Phys. Rev. C* 84 (2011) 054316.
- [5] I. Hamamoto, B.R. Mottelson, *Phys. Lett. B* 127 (1983) 281.
- [6] I. Hamamoto, B.R. Mottelson, *Phys. Lett. B* 132 (1983) 7.
- [7] I. Hamamoto, *Phys. Lett. B* 193 (1987) 399.
- [8] G.J. Lane, et al., *Phys. Rev. C* 82 (2010) 051304.
- [9] G.D. Dracoulis, et al., *Phys. Lett. B* 709 (2012) 59.
- [10] C. Bihari, et al., *Phys. Scr.* 78 (2008) 045201.
- [11] P. Sarriguren, R. Rodríguez-Guzán, L.M. Robledo, *Phys. Rev. C* 77 (2008) 064322.
- [12] J.M. Allmond, et al., *Phys. Rev. C* 78 (2008) 014302.
- [13] K. Nomura, et al., *Phys. Rev. Lett.* 108 (2012) 132501.
- [14] J. Meyer-Ter-Vehn, *Nucl. Phys. A* 249 (1975) 111.
- [15] J. Meyer-Ter-Vehn, *Nucl. Phys. A* 249 (1975) 141.
- [16] A.S. Davydov, G.F. Flhppov, *Nucl. Phys.* 8 (1958) 237.
- [17] R. Bengtsson, H. Frisk, F.R. May, J.A. Pinston, *Nucl. Phys. A* 415 (1984) 189.
- [18] I. Hamamoto, B.R. Mottelson, *Phys. Lett. B* 167 (1986) 370.
- [19] G.B. Hagemann, I. Hamamoto, *Phys. Rev. C* 40 (1989) 2862.
- [20] R. Broda, *J. Phys. G* 32 (2006) R151.
- [21] R.V.F. Janssens, F.S. Stephens, *Nucl. Phys. News* 6 (1996) 9.
- [22] C.R. Hirling, D.G. Burke, *Can. J. Phys.* 54 (1976) 1360.
- [23] C.R. Hirling, D.G. Burke, E.R. Flynn, J.W. Sunier, P.A. Schmelzbach, R.F. Haglund Jr, *Nucl. Phys. A* 287 (1977) 24.
- [24] T. Shizuma, et al., *Eur. Phys. J. A* 17 (2003) 159.
- [25] M. Caamaño, et al., *Eur. Phys. J. A* 23 (2005) 201.
- [26] S.J. Steer, et al., *Phys. Rev. C* 84 (2011) 044313.
- [27] T. Kibédi, T.W. Burrows, M.B. Trzhaskovskaya, P.M. Davidson, C.W. Nestor Jr., *Nucl. Instrum. Methods A* 589 (2008) 202.
- [28] R.B. Firestone, *Table of Isotopes*, John Wiley and Sons, New York, 1996.
- [29] M.W. Reed, et al., to be published.
- [30] S.E. Larsson, G. Leander, I. Ragnarsson, *Nucl. Phys. A* 307 (1978) 189.
- [31] P. Möller, J.R. Nix, W.D. Myers, W.J. Swiatecki, *At. Data Nucl. Data Tables* 59 (1995) 185.
- [32] A. Bohr, B.R. Mottelson, *Nuclear Structure*, W.A. Benjamin Inc., 1975.